

NIR SPECTROMETER FOR BUNCH-RESOLVED, NON-DESTRUCTIVE STUDIES OF MICROBUNCHING AT EUROPEAN XFEL

S. Fahlström, M. Hamberg, Uppsala University, Uppsala, Sweden
Ch. Gerth*, N. M. Lockmann, B. Steffen, DESY, Hamburg, Germany

Abstract

At the European X-ray Free Electron Laser high brilliance femtosecond FEL radiation pulses are generated for user experiments. For this to be achieved, electron bunches must be reliably produced within very tight tolerances. In order to investigate the presence of microbunching, i.e. charge density variation along the electron bunch with features in the micron range, a prism-based NIR spectrometer with an InGaAs sensor, sensitive in the wavelength range 900 nm to 1700 nm was installed. The spectrometer utilizes diffraction radiation (DR) generated at electron beam energies of up to 17.5 GeV. The MHz repetition rate needed for bunch resolved measurements is made possible by the KALYPSO line detector system, providing a read-out rate of up to 2.7 MHz. We present the first findings from commissioning of the NIR spectrometer, and measurements on the impact of the Laser Heater system for various bunch compression settings, in terms of amplitude and bunch-to-bunch variance of the NIR spectra as well as FEL pulse energy.

INTRODUCTION

The European XFEL

In the linear accelerator of the European X-ray Free-Electron Laser (EuXFEL) electron bunches are accelerated to energies of up to 17.5 GeV. The bunches are accelerated in bunch trains of up to 2700 bunches, with an intra-train repetition rate of up to 4.5 MHz (currently 1.1 MHz operation is most common). Trains are generated at 10 Hz, for a total of up to 27 000 bunches per second.[1] After acceleration, the electron bunches are distributed to three undulator sections (designated SASE1, SASE2, and SASE3) where via Self-Amplified Spontaneous Emission (SASE) laser-like X-rays are produced. This enables parallel Free-Electron Laser (FEL) operation of three experimental stations.

Bunch Compression

The peak currents needed for the SASE process demand that the bunches are longitudinally compressed during acceleration. To compress the bunches a longitudinal energy-position correlation called *chirp* is imparted by accelerating them off crest and then leading them through a chicane where energy dependent path length allows the higher energy tail to catch up to the head. At the EuXFEL this is done in 3 stages, for a total compression factor of ~ 100 , and final peak current ~ 5 kA. [2]

Microbunching and Laser Heater

Collective effects during bunch compression can lead to so called *microbunches* developing [3, 4], where random periodic features on the longitudinal charge density from shot noise from the electron-gun can be amplified many orders of magnitude. These features lead to growth of slice emittance, detrimental to the FEL process. Previously similar facilities have implemented Laser Heaters (LH) to inhibit microbunching, with clear improvements to FEL performance.[5–7] In the LH, part of the laser pulse for the photo-cathode electron gun is coupled out and overlapped with the electron bunches in an undulator inside a chicane. This imparts a non-correlated energy spread, which dampens microbunching in the bunch compressor chicanes. A LH was also installed at the EuXFEL.[8–12]

Longitudinal Diagnostics of Short Bunches

For the study of microbunching effects at the EuXFEL a prism based Near Infra-red (NIR) spectrometer was installed.

For longitudinal diagnostics of sub picosecond electron bunches, frequency domain methods using coherent radiation can provide a non-invasive option, important for user facilities. The spectral density of coherent radiation is dependent on the magnitude of the longitudinal form factor, F_L , which is the Fourier transform of the longitudinal charge density of the electron bunch. Coherent Diffraction Radiation (CDR) spanning mm-waves to visible light is generated when the relativistic electron bunches pass through a hole in an aluminum screen. At EuXFEL this CDR is used to non-invasively monitor bunch compression and longitudinal profiles at several stations along the accelerator. [13] Bunch Compression Monitors (BCM) use simple and robust broadband sensors to monitor the overall bunch length. Spectroscopic investigation offer a more complete bunch profile, and at the last CDR station, after full acceleration, a THz spectrometer [14, 15] was previously installed.[16] That spectrometer works in the mid infrared (MIR) to THz spectral range, $5 \mu\text{m}$ to $450 \mu\text{m}$, and can provide complete bunch profiles. However, the smallest features it can resolve is limited by its detection range. Since microbunching is suspected with features in the single μm range, the spectrometer that this paper concerns was installed alongside it, sensitive in the NIR range. Due to the stochastic origins of microbunching great variance from bunch to bunch is expected, which requires bunch-resolved measurements. The development of the KALYPSO detector unit [17–20] has made this possible, with read-out rates up to 2.7 MHz.

* christopher.gerth@desy.de

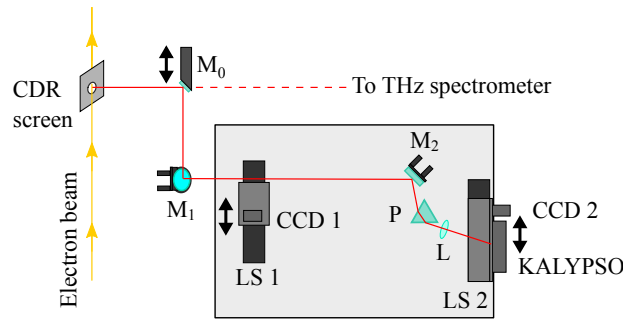


Figure 1: Layout of the NIR spectrometer. Not to scale.

NIR SPECTROMETER

The layout of the NIR spectrometer is shown in Fig. 1. The KALYPSO detector module has a 256 pixel InGaAs line sensor sensitive to $0.9\ \mu\text{m}$ to $1.7\ \mu\text{m}$. The sensor is 12.8 mm wide, with a pixel pitch of $50\ \mu\text{m}$. The NIR spectrometer also has two Si CCD cameras, CCD1 and CCD2, for alignment and CDR beam profile imaging.

A 60 mm equilateral n-SF11 prism is used for dispersion. The n-SF11 glass has a relatively flat slope for the sought spectral range. A 2" n-BK7, $f = 150\ \text{mm}$ plano-convex lens is used for focusing. To compensate for the shift of focal length due to decreasing refractive index for longer wavelengths, the central wavelength is incident on the sensor at an angle off of the normal.

The NIR spectrometer is assembled on a standard optical breadboard. Two 2" mirrors, M1 and M2, mounted on 2-axis Standa motorized mirror mounts, are used for alignment. Two linear stages are mounted on the breadboard, LS1 and LS2. LS1 holds CCD1 and has extra space where e.g. optical filters for calibration purposes can be mounted. LS2 holds the KALYPSO detector module and CCD2.

INITIAL FINDINGS

We present measurements for scans over bunch compression, and LH power from three different measurement runs at different compression settings and FEL operation. Accelerator parameters are presented in Table 1. For the third LH scan run, the accelerator was operated in so-called flattop mode, where two different compression settings can be applied for different ranges of bunches within the same bunch train. Our read-out script was however only able to record the compression settings of the first flattop range. No FEL operation during 3rd run. Points in plots are averages over many bunch trains, and the standard deviation is indicated with error bars or transparent bands.

Changing Compression Settings

Figure 2 shows example spectra from the first readings with the NIR spectrometer. Uncompressed bunches in the left column and bunches at FEL compression settings in the right. The overall intensity decreased by almost 2 orders of magnitude when the bunches were compressed. This is in

Table 1: Accelerator Parameters for LH Measurement Runs

Run	1st acc. section		2nd acc. section	
	ΔE [MeV]	chirp [1/m]	ΔE [MeV]	chirp [1/m]
1	128.9	-9.04	569.8	-10.85
2	128.4	-8.67	579.2	-10.50
3a*	127.6	-8.65	585.4	-10.49

*Accelerator operated in "flattop" mode.

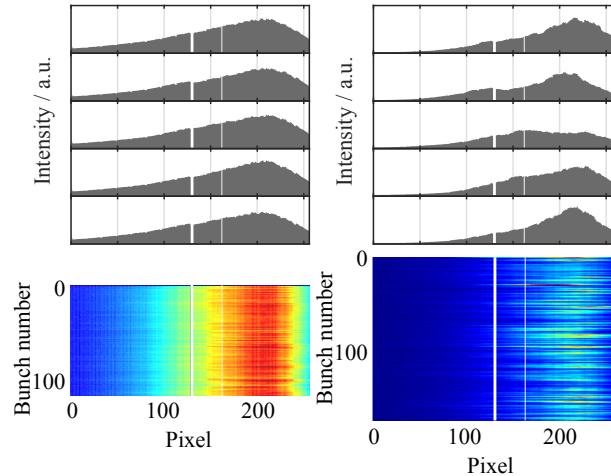


Figure 2: Example spectra from initial measurements with the NIR spectrometer. Longer wavelengths towards higher pixel number (uncalibrated). Left column: uncompressed beam. Right column: FEL compression settings. Top row: Selected spectra. N.B. vertical scales differ: compressed signal ~ 100 times weaker. Bottom row: Whole bunch trains, demonstrates differences in shot-to-shot fluctuations.

line with earlier results from FLASH, where microbunching was observed in the μm range for lower compression settings.[21] With FEL compression the relative bunch-to-bunch variance increased.

Scans over the chirp of the accelerator sections in the first two compression stages were made. The results are shown in Fig. 3. The signal of the NIR spectrometer was split in two halves, integrated and then normalized separately to show the shift of the spectrum during the scan. In black the BCM signal is shown, corresponding to right y-axis. We can see that the decrease in NIR intensity continues after maximum compression is reached. A general dampening occurs of development of features in the μm range in the chicanes.

Changing Laser Heater Power

Figure 4 shows NIR spectrometer and FEL intensities from run 1 and 2. Only SASE1 was operational for run 1. We see an expected behavior, the NIR intensity falls off and the FEL intensity generally sees an initial increase before the induced energy spread from the LH becomes too large. For all except SASE3 during run 2, the increase in intensity is

Content from this work may be used under the terms of the CC BY 3.0 licence (© 2019). Any distribution of this work must maintain attribution to the author(s), title of the work, publisher, and DOI

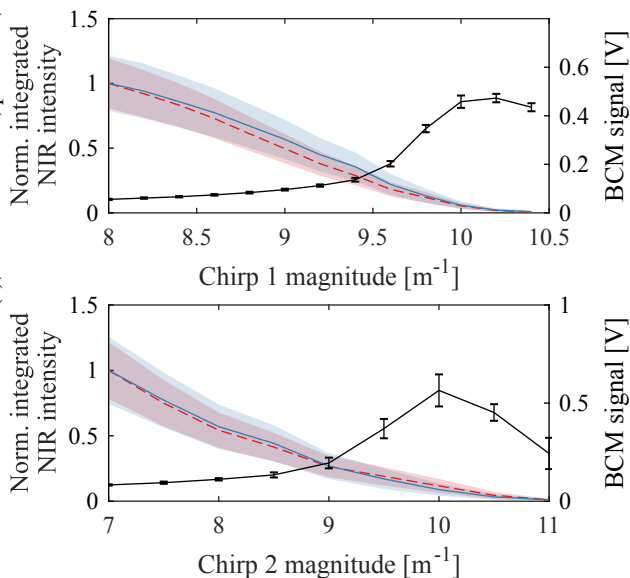


Figure 3: Scans over bunch compression. Left axes: Signal from NIR spectrometer integrated and normalized separately for pixel 0-127 (dashed red line) and 128-255 (solid blue line). Transparent regions indicate the standard deviation. Right axes: Signal from BCM, black line with error bars. Top: Compression adjusted with accelerator chirp before first chicane. Bottom: Adjusted using chirp between first and second chicane.

significant. However, in none of the cases the FEL intensity is higher than what has been achieved without the LH.

Figure 5 shows the NIR intensities for all runs. Run 3 went to higher LH pulse energies, and a difference in behaviour between flattop ranges is seen for these higher energies, with flattop one exhibiting an unexpected increase in intensity and variance.

CONCLUSION

We have shown the first commissioning results from a new NIR spectrometer with bunch-to-bunch read-out capabilities at MHz repetition rates.

The investigations of compression settings show a behaviour in line with previous findings[21] where significant microbunching occurs in the chicanes at lower compression, while with increased chirp microbunching is strongly suppressed, due to longitudinal smearing by the energy distribution inside the bunch. Shot-to-shot variance with high compression suggests that some microbunching could still remain.

LH investigations show some positive effects on the FEL pulse energy for moderate LH pulse energies. The effect is not as significant as in other FEL facilities where the LH is necessary for regular operation, whereas so far at EuXFEL full FEL performance could be achieved without using the LH. Reasons for this could be, for instance, different properties of the photo-cathode material in the electron-gun for

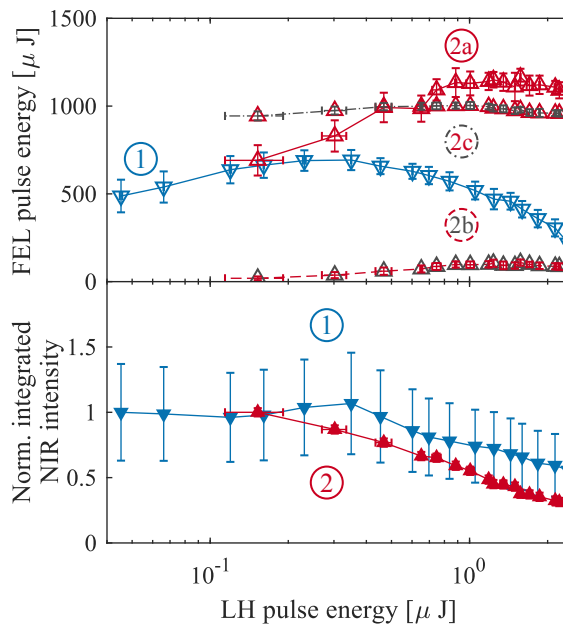


Figure 4: Results from scan of LH pulse energy from Runs 1 and 2. Top: FEL pulse energy. 2a - SASE1, 2b - SASE2, 2c - SASE3. Bottom: Integrated signal across all pixels, normalized with regards to their initial values.

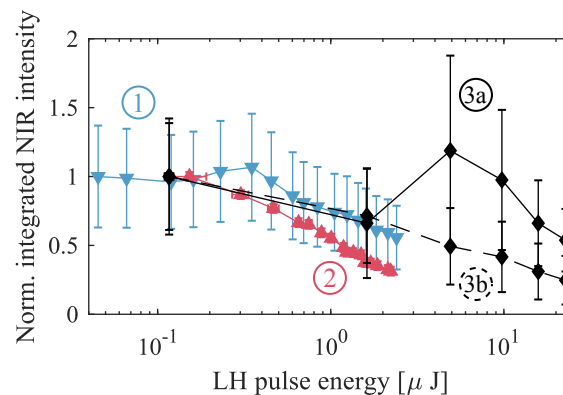


Figure 5: Results from scan of LH pulse energy from all runs. Run 3 was made during "flattop" operation mode, and also to higher LH pulse energies. 3a is flattop 1 (first 100 bunches), 3b is flattop 2 (bunch 160 and onward).

the generation of the electron bunches, or beam dynamics of the entire accelerator not producing microbunching with as high gain for features in the micrometer wavelength range.

ACKNOWLEDGEMENTS

The authors are deeply grateful to all people who contributed to bring European XFEL into successful operation. The authors would also like to thank F. Brinker (DESY) for the support during LH power scans and fruitful discussions, and V. Rybnikov (DESY) for software support with the KALYPSO detector and CCD cameras.

REFERENCES

- [1] M. O. Wiedorn *et al.*, “Megahertz serial crystallography,” *Nat. Commun.*, vol. 9, no. 1, p. 4025, Oct. 2018, ISSN: 2041-1723. DOI: 10.1038/s41467-018-06156-7.
- [2] G. Feng *et al.*, “Beam dynamics simulations for european xfel,” DESY, Tech. Rep., 2013, TELSAs-FEL 2013-04.
- [3] E. L. Saldin, E. A. Schneidmiller, and M. Yurkov, “Klystron instability of a relativistic electron beam in a bunch compressor,” *Nucl. Instrum. Methods Phys. Res., Sect. A*, vol. 490, no. 1-2, pp. 1–8, 2002. DOI: 10.1016/S0168-9002(02)00905-1.
- [4] E. L. Saldin, E. A. Schneidmiller, and M. Yurkov, “Longitudinal space charge-driven microbunching instability in the tesla test facility linac,” in *Free Electron Lasers 2003*, Elsevier, 2004, pp. 355–359. DOI: 10.1016/j.nima.2004.04.067.
- [5] Z. Huang *et al.*, “Suppression of microbunching instability in the linac coherent light source,” *Phys. Rev. Spec. Top. Accel Beams*, vol. 7, no. 7, p. 074401, 2004. DOI: 10.1103/PhysRevSTAB.7.074401.
- [6] Z. Huang *et al.*, “Measurements of the linac coherent light source laser heater and its impact on the x-ray free-electron laser performance,” *Phys. Rev. Spec. Top. Accel Beams*, vol. 13, no. 2, pp. 1098–1103, 2010. DOI: 10.1103/PhysRevSTAB.13.020703.
- [7] S. Spampinati *et al.*, “Laser heater commissioning at an externally seeded free-electron laser,” *Phys. Rev. Spec. Top. Accel Beams*, vol. 17, p. 120705, 12 Dec. 2014. DOI: 10.1103/PhysRevSTAB.17.120705.
- [8] M. Hamberg, V. Ziemann, *et al.*, “Status of the eu-xfel laser heater,” in *Proc. 35th Int. Free Electron Laser Conf. (FEL'13)*, paper TUPSO25, New York, NY, USA, 2013, p. 5.
- [9] M. Hamberg and V. Ziemann, “Progress of the eu-xfel laser heater,” in *Proc. 5th Int. Particle Accelerator Conf. (IPAC'14)*, JACoW, Geneva, Switzerland, Dresden, Germany, 2014, pp. 2912–2913. DOI: 10.18429/JACoW-IPAC2014-THPR0024.
- [10] M. Hamberg and V. Ziemann, “Construction of the EU-XFEL Laser Heater,” in *Proc., 37th Int. Free Electron Laser Conf. (FEL'15)*, Daejeon, Korea, 2015, TUP038. DOI: 10.18429/JACoW-FEL2015-TUP038.
- [11] M. Hamberg, F. Brinker, and M. Scholz, “First Heating with the European XFEL Laser Heater,” in *Proc. 5th Int. Beam Instrumentation Conf. (IBIC'16)*, Barcelona, Spain, 2016, WEPG32. DOI: 10.18429/JACoW-IBIC2016-WEPG32.
- [12] M. Hamberg *et al.*, “Electron beam heating with the european xfel laser heater,” in *Proc. 38th Int. Free Electron Laser Conf.*, Santa Fe, NM, USA, 2017, pp. 458–459. DOI: 10.18429/JACoW-FEL2017-WEP018.
- [13] P. Peier, C. Gerth, and H. Dinter, “Coherent radiation diagnostics for longitudinal bunch characterization at european xfel,” in *Proc. 36th Int. Free Electron Laser Conf. (FEL'14)*, paper THP083, 2014.
- [14] S. Wesch, B. Schmidt, C. Behrens, H. Delsim-Hashemi, and P. Schmüser, “A multi-channel thz and infrared spectrometer for femtosecond electron bunch diagnostics by single-shot spectroscopy of coherent radiation,” *Nucl. Instrum. Methods Phys. Res., Sect. A*, vol. 665, pp. 40–47, 2011. DOI: 10.1016/j.nima.2011.11.037.
- [15] B. Schmidt *et al.*, “Longitudinal bunch diagnostics using coherent transition radiation spectroscopy. physical principles, multichannel spectrometer, experimental results, mathematical methods,” Deutsches Elektronen-Synchrotron (DESY), Tech. Rep., 2018. DOI: 10.3204/PUBDB-2018-01372.
- [16] N. Lockmann, C. Gerth, P. Peier, B. Schmidt, S. Wesch, *et al.*, “A non-invasive thz spectrometer for bunch length characterization at european xfel,” in *Proc. 10th Int. Particle Accelerator Conf. (IPAC'19)*, Melbourne, Australia, 2019, pp. 2495–2497. DOI: 10.18429/JACoW-IPAC2019-WEPGW014.
- [17] L. Rota *et al.*, “A high-throughput readout architecture based on pci-express gen3 and directgma technology,” *J. Instrum.*, vol. 11, no. 02, P02007, 2016. DOI: 10.1088/1748-0221/11/02/P02007.
- [18] L. Rota *et al.*, “Kalypso: A mfps linear array detector for visible to nir radiation,” in *Proc. 5th Int. Beam Instrumentation Conf. (IBIC'16)*, Barcelona, Spain, 2016, pp. 740–743. DOI: 10.18429/JACoW-IBIC2016-WEPG46.
- [19] L. Rota *et al.*, “Kalypso: Linear array detector for high-repetition rate and real-time beam diagnostics,” *Nucl. Instrum. Methods Phys. Res., Sect. A*, 2018. DOI: 10.1016/j.nima.2018.10.093.
- [20] M. Caselle *et al.*, “Ultra-fast detector for wide range spectral measurements,” in *Proc. Real-time Meas., Rogue Phenomena, and Single-Shot Appl. IV*, International Society for Optics and Photonics, vol. 10903, San Francisco, California, United States, 2019, p. 1 090 306. DOI: 10.1117/12.2511341.
- [21] S. Wesch, C. Behrens, B. Schmidt, and P. Schmüser, “Observation of coherent optical transition radiation and evidence for microbunching in magnetic chicanes,” in *Proc. 31st Int. Free Electron Laser Conf. (FEL'09)*, (Liverpool, UK), paper WEP50, 2009, pp. 619–622.